

Joint ML-Bayesian Approach to Adaptive Radar Detection in the presence of Gaussian Interference

Chaoran Yin
Tianqi Wang
Linjie Yan

Chengpeng Hao, Senior Member, IEEE
Institute of Acoustics,
Chinese Academy of Sciences, Beijing, 100190, China

Alfonso Farina, Life Fellow, IEEE
Selex ES (retired), a consultant, Roma, Italy

Danilo Orlando, Senior Member, IEEE
Dipartimento di Ingegneria dell'Informazione, Universita di Pisa, Via
Caruso 16, 56122 Pisa, Italy

Abstract—This paper addresses the adaptive radar target detection problem in the presence of Gaussian interference with unknown statistical properties. To this end, the problem is first formulated as a binary hypothesis test, and then we derive a detection architecture grounded on the hybrid of Maximum Likelihood (ML) and Maximum A Posteriori (MAP) approach. Specifically, we resort to the hidden discrete latent variables in conjunction with the Expectation-Maximization (EM) algorithms which cyclically updates the estimates of the unknowns. In this framework, the estimates of the *a posteriori* probabilities under each hypothesis are representative of the inherent nature of data and used to decide for the presence of a potential target. In addition, we prove that the developed detection scheme ensures the desired Constant False Alarm Rate property with respect to the unknown interference covariance matrix. Numerical examples obtained through synthetic and real recorded data corroborate the effectiveness of the proposed architecture and show that the

This work was supported by the National Natural Science Foundation of China under Grant 62201564. The work of D.Orlando was partially supported by the Italian Ministry of Education and Research (MUR) in the framework of the FoReLab project (Departments of Excellence) and in part by the European Union in the NextGenerationEU plan through the Italian program “Bando PRIN 2022”, D.D. 104/2022 (PE7, project “CIRCE,” code H53D23000420006). (*Corresponding author: Chengpeng Hao*).

Chaoran Yin, Tianqi Wang, Linjie Yan, and Chengpeng Hao are with the Institute of Acoustics, Chinese Academy of Sciences, Beijing 100190, China, (e-mail: yinchaoran18@mails.ucas.ac.cn, wangtianqi@mail.ioa.ac.cn, yanlinjie16@163.com, haohengp@mail.ioa.ac.cn); Alfonso Farina is with Selex ES (retired), a consultant, Roma, Italy. (e-mail: alfonso.farina@outlook.it); Danilo Orlando is with Dipartimento di Ingegneria dell'Informazione, Universita di Pisa, Via Caruso 16, 56122 Pisa, Italy. (e-mail: danilo.orlando@unipi.it);

MAP-based approach ensures evident improvement with respect to the conventional generalized likelihood ratio test at least for the considered scenarios and parameter setting.

Index Terms—clutter suppression, covariance matrix estimation, expectation maximization, maximum a posteriori probability, radar, target detection

I. Introduction

IN the course of the last century, radar systems are becoming increasing ubiquitous and affect many aspects of real life. As a consequence, adaptive radar target detection in the presence of Gaussian background with unknown statistical properties has been addressed for decades [1]. Based on the well-known Neyman-Pearson criterion [2], a plethora of solutions can be found in the open literature, especially detection architectures devised under increasingly challenging working scenarios due to the development of electronic technology in the last years. In the seminal paper by Kelly [3], the related binary hypothesis testing problem is solved by means of the Generalized Likelihood Ratio Test (GLRT), which consists in comparing likelihood ratio to a threshold corresponding to a pre-assigned False Alarm Probability (P_{fa}); the unknown parameters are replaced by their maximum likelihood estimates. The GLRT enjoys the desired Constant False Alarm Rate (CFAR) property with respect to the background and uses a set of secondary data, free of target components and sharing the same interference characterization as that in the Cell Under Test (CUT). An *ad hoc* modification of the GLRT is devised in [4] under the assumption that the covariance of the Gaussian interference is perfectly known and then replaced by the sample covariance matrix formed using the secondary data. The Adaptive Matched Filter (AMF) developed in [4] reduces significantly the computational load at the cost of a slight degradation of the detection performance with respect to the GLRT. This result inspired a continuous investigation of several approaches in the radar community also considering that there do not exist Uniformly Most Powerful (UMP) detectors for this problem [5].

As a matter of fact, the detection performance of the GLRT and AMF heavily depends on the quality of the estimates of Clutter Covariance Matrix (CCM). In this respect, the knowledge-aided framework has been proposed which consists in exploiting prior knowledge about the systems and/or background at the design stage. For example, the symmetry of the antenna array or pulse trains is widely considered, which leads to a persymmetric CCM that is Hermitian with respect to the diagonal and symmetric with respect to the counter-diagonal [6]–[12]. This specific structure greatly reduces the unknown parameters in the matrix and thus allows for enhancement of the estimation quality for a given number of secondary data. As an alternative approach, symmetric spectrum detectors are derived by exploiting the CCM in real domain that arises when the power spectrum density of

the received clutter is symmetric with respect to zero after compensation for the Doppler frequency [13]–[15]. It is important to notice that the above knowledge-aided detectors enjoy reliable detection performance in the *sample-starved* situations [16], [17] where the volume of uniform secondary data is limited and the conventional detectors significantly impair their performance [18].

Another approach used to capitalize the target energy consists in taking into account the fact that target components are present in adjacent range/Doppler bins (spillover) [19]. This energy contamination is due to the mismatch between the sampling point and the true position of the target and, consequently, the latter straddles between two consecutive cells, possibly causing significant signal power loss in the CUT. In [19], the authors first develop the spillover architecture using continuous range bins and come up with three detectors based on one-step and two-step GLRT that are capable of joint detection and localization of a target within the CUT. It has been verified that when the mismatch occurs, the detectors devised under the assumption outperform the counterparts and provide accurate target range estimation within a given range cell [20]–[23]. This architecture is extended to the range-Doppler plane for Multi-Input Multi-Output radar in [24], wherein an *ad hoc* approximation of the GLRT is adopted due to complex mathematics. It is also worth mentioning that knowledge-aided spillover detectors are obtained in [20], [21] to further enhance the robustness of the systems.

Subspace signal model represents another viable mean to deal with the mismatch and target energy loss in radar operating scenarios [25], [26]. In fact, such paradigm arises from the desire to cope with the uncertainty related to the radar array steering direction caused by, for example, unbalanced channels, miscalibration errors, and mutual coupling [27]–[29], and mitigate the energy degradation in the presence of signal mismatches. In this framework, the uncertainty is accounted for by the unknown coordinates of a signal that lies in a subspace (perfectly known or known only by the dimension) [30]–[37]. In [26] and [38], the authors derive several detectors based on GLRT for both unconstrained coordinates (first-order) and constrained coordinates by a prior distribution (second-order), and accordingly establish a unified framework for adaptive subspace detection. The subspace detectors are desirable when radar is working on the searching mode [29] due to a certain level of tolerance for target mismatch (robustness). On the other hand, selective detectors such as Rao test [39], [40], which are sensitive to the mismatch and tend to reject the target misaligned with the nominal steering vector, are preferable in target localization. In [41], the problem of designing robust or selective detectors is addressed by deriving the decision region boundary of the clustered data in a suitable plane formed by maximal invariants [42]. In particular, it is shown that the selective detector can be obtained without sacrificing detection performance under matched conditions.

Observe that the above detection architectures share the common assumption that the unknown parameters are considered deterministic. As an alternative, the Bayesian approach consists in assuming that the unknowns are random variables and obey *a priori* distributions [43]–[46]. Such a line of reasoning leads to the so-called *a posteriori* distributions and has been widely applied in radar target detection. For example, [5] assumes that the CCM is inverse Wishart distributed and develops three Bayesian detectors based on the GLRT. As a consequence, the prior knowledge is included via a colored-loading and greatly improves the parameter estimation performance. The effectiveness is corroborated through extensive examples conducted on simulation and real recorded databases. In [47], Bayesian parametric detectors are devised by assuming *a priori* distribution for the noise in an auto-regressive process. For cognitive radar [48], Bayesian method is an alternative in the decision-action phase which adaptively optimizes the transmitted waveform according to the knowledge perceived from the background [49]. Furthermore, as indicated in [50], the Bayesian approach can also be used to learn the specific structure of the unknown CCM, which is a preliminary step for applying the knowledge-aided detectors mentioned before. Given the advantages of the Bayesian philosophy, [51] proposes a Maximum A Posterior (MAP) test for target detection which compares the ratio of *a posteriori* distributions maximized over joint parameter and hypothesis space with a threshold set according to the false alarm rate. Illustrative examples show that the detector performs significantly better than the GLRT-based detectors.

Therefore, recalling that a UMP test for the fundamental problem defined in [3] does not exist and encouraged by the aforementioned efforts towards more and more powerful decision rules, in this paper, we provide an innovative solution to the conventional adaptive detection problem by resorting to a joint Bayesian and Maximum Likelihood (ML) approach. Unlike [51], we do not require any *a priori* information about the unknown parameters and the *a posteriori* probabilities are iteratively obtained by applying the Expectation-Maximization (EM) algorithm [52]–[55]. Specifically, we introduce a fictitious discrete random variable [43] that represents the status of the CUT for what concerns the target presence. This random variable is not observable and its value assigns a label (or class) to the CUT. Thus, we modify the original data distribution in order to account for this hidden random variable and estimate the corresponding unknown parameters through the EM. This line of reasoning allows us to obtain the estimates of the *a posteriori* probabilities that the hidden class takes on a value given the data from the CUT. Such probabilities can then be used to devise a decision scheme grounded on the minimization of the Bayes risk and that exploits the ML-based estimates returned by the EM algorithm. Remarkably, we demonstrate that the proposed decision scheme ensures the CFAR property with respect to the

interference covariance matrix. The main contributions of this paper are

- the design of a joint Bayesian-ML detection architecture that allows for a control of the P_{fa} through a suitable parameter. Notice also that the proposed approach can be considered as a generalization of the MAP design criterion;
- the application of the EM algorithm to estimate the unknown parameters used to build up the decision scheme;
- a formal proof of the CFAR property of the proposed detector showing that the invariance with respect to the interference covariance matrix holds true when the iterative procedure starts from suitable initial values.

The remainder of the paper is organized as follows. The next section is devoted to the problem formulation, whereas the Section III contains the detection architecture design and parameter estimation procedures. Section IV analytically demonstrates the CFAR property of the proposed architecture, while illustrative examples and the related discussion are given in Section V. Finally, in Section VI, we draw some concluding remarks and present possible future work routes.

A. Notation

In what follows, vectors (matrices) are denoted by boldface lower (upper) case letter. Superscripts $(\cdot)^T$ and $(\cdot)^\dagger$ denote transpose and complex conjugate transpose, respectively. \mathbf{I}_N stands for an identity matrix of size $N \times N$. $\nu(\mathbf{M})$ is the vector containing the general distinct entries of the matrix \mathbf{M} . The notation \sim means “is distributed as”. $\mathcal{CN}_N(\boldsymbol{\mu}, \mathbf{X})$ denotes the N -dimensional circular complex Gaussian distribution with mean $\boldsymbol{\mu}$ and positive-definite covariance matrix \mathbf{X} . $P(c = m)$ stands for the probability that a discrete random variable c equals to m . $\mathcal{CW}(K, N; \mathbf{I}_N)$ denotes the N -dimensional complex Wishart distribution with K degrees of freedom and scale matrix \mathbf{I}_N . $\det(\cdot)$ and $\text{Tr}(\cdot)$ represent the determinant and trace of a matrix, respectively. $|\cdot|$ denotes the modulus of a scalar. The symbol $\mathbf{0}$ denotes a matrix or vector of zeros of proper dimensions. As for the numerical sets, \mathbb{C} is the set of complex numbers and $\mathbb{C}^{N \times M}$ is the Euclidean space of $(N \times M)$ -dimensional complex matrices (or vectors, if $M = 1$).

II. Problem Formulation and EM-based Estimation

Let us assume a radar system equipped with $N \geq 2$ time and/or space channels. The echoes of the transmitted waveform from the region of interest are properly collected, sampled, and processed to form several N dimensional vectors representative of consecutive range bins. We denote by $\mathbf{z} \in \mathbb{C}^{N \times 1}$ the signal vector corresponding to the CUT and we want to decide whether or not it contains target component. To this end, the signal

vectors in the neighbourhood of the CUT, denoted by $\mathbf{z}_1, \dots, \mathbf{z}_K \in \mathbb{C}^{N \times 1}$, are utilized as secondary data¹ to estimate the interference statistical properties. Then, the radar target detection problem can be formulated as a binary hypothesis test, i.e.,

$$\begin{cases} H_0 : \begin{cases} \mathbf{z} = \mathbf{n}, \\ \mathbf{z}_k = \mathbf{n}_k, k = 1, \dots, K, \end{cases} \\ H_1 : \begin{cases} \mathbf{z} = \alpha \mathbf{v} + \mathbf{n}, \\ \mathbf{z}_k = \mathbf{n}_k, k = 1, \dots, K, \end{cases} \end{cases} \quad (1)$$

where $\mathbf{n}, \mathbf{n}_k, k = 1, \dots, K$, are the interference component modeled as statistically independent circular complex Gaussian distributed variables with zero mean and covariance matrix $\mathbf{M} \in \mathbb{C}^{N \times N}$, α stands for the unknown complex amplitude of target echo, and $\mathbf{v} \in \mathbb{C}^{N \times 1}$ is the nominal steering vector. Denote by $\mathbf{Z} = [\mathbf{z}, \mathbf{z}_1, \dots, \mathbf{z}_K] \in \mathbb{C}^{N \times (K+1)}$ the overall data matrix, then the Probability Density Function (PDF) of \mathbf{Z} under H_0 and H_1 is given by

$$f_0(\mathbf{Z}; \boldsymbol{\theta}_0) = \left[\frac{1}{\pi^N \det(\mathbf{M})} \right]^{(K+1)} \exp \{ -\text{Tr} [\mathbf{M}^{-1} \mathbf{Z} \mathbf{Z}^\dagger] \}, \quad (2)$$

$$f_1(\mathbf{Z}; \boldsymbol{\theta}_1) = \left[\frac{1}{\pi^N \det(\mathbf{M})} \right]^{(K+1)} \times \exp \{ -\text{Tr} [\mathbf{M}^{-1} ((\mathbf{z} - \alpha \mathbf{v})(\mathbf{z} - \alpha \mathbf{v})^\dagger + \mathbf{S})] \}, \quad (3)$$

respectively, where $\boldsymbol{\theta}_0 = \nu(\mathbf{M})$, $\boldsymbol{\theta}_1 = [\alpha, \boldsymbol{\theta}_0^T]^T$, and $\mathbf{S} = \mathbf{K} \mathbf{S}'$ with $\mathbf{S}' = \frac{1}{K} \sum_{k=1}^K \mathbf{z}_k \mathbf{z}_k^\dagger$ the sample covariance matrix based upon secondary data.

Let us now introduce a latent variable c , whose Probability Mass Function (PMF) is $P(c = t) = p_t > 0$, $t = 0, 1$, with $p_0 + p_1 = 1$. Moreover, we assume that when $c = 0$, then $\alpha = 0$, whereas if $c \neq 0$, then $\alpha \neq 0$. It follows that the PDF of \mathbf{Z} can be recast as

$$f(\mathbf{Z}; \boldsymbol{\delta}) = p_0 f_0(\mathbf{Z}; \boldsymbol{\theta}_0) + p_1 f_1(\mathbf{Z}; \boldsymbol{\theta}_1), \quad (4)$$

where $\boldsymbol{\delta} = [p_0, p_1, \boldsymbol{\theta}_0^T, \boldsymbol{\theta}_1^T]^T$. It turns out that the PDF of \mathbf{Z} becomes a convex linear combination of the PDFs under H_0 and H_1 . In this context, since c is not observable, it is difficult to estimate its PMF through the maximum likelihood approach and, hence, we estimate the unknown parameters of $f(\mathbf{Z}; \boldsymbol{\delta})$ by resorting to the EM algorithm which iteratively provides closed-form estimate updates towards at least one local stationary point. More precisely, in the cyclic optimization procedure of the EM algorithm, the l th iteration contains two steps referred to as E-step and M-step [54], [55], respectively. The E-step leads to the computation of the *a posteriori* probabilities of each hypothesis given \mathbf{Z} , namely,

$$q_0^{(l-1)}(\mathbf{Z}) = \frac{\hat{p}_0^{(l-1)} f_0(\mathbf{Z}; \hat{\boldsymbol{\theta}}_0^{(l-1)})}{\hat{p}_0^{(l-1)} f_0(\mathbf{Z}; \hat{\boldsymbol{\theta}}_0^{(l-1)}) + \hat{p}_1^{(l-1)} f_1(\mathbf{Z}; \hat{\boldsymbol{\theta}}_1^{(l-1)})}, \quad (5)$$

$$q_1^{(l-1)}(\mathbf{Z}) = \frac{\hat{p}_1^{(l-1)} f_1(\mathbf{Z}; \hat{\boldsymbol{\theta}}_1^{(l-1)})}{\hat{p}_0^{(l-1)} f_0(\mathbf{Z}; \hat{\boldsymbol{\theta}}_0^{(l-1)}) + \hat{p}_1^{(l-1)} f_1(\mathbf{Z}; \hat{\boldsymbol{\theta}}_1^{(l-1)})}, \quad (6)$$

¹Notice that secondary data \mathbf{z}_k s are assumed free of target components regardless which hypothesis is in force.

with $\hat{p}_0^{(l-1)}$, $\hat{\theta}_0^{(l-1)}$, $\hat{p}_1^{(l-1)}$ and $\hat{\theta}_1^{(l-1)}$ being the estimates of p_0 , θ_0 , p_1 and θ_1 , at the $(l-1)$ th iteration, respectively. As for the M-step, it consists in solving the following optimization problem

$$\hat{\delta}^{(l)} = \arg \max_{\delta} \left\{ \sum_{t=0}^1 q_t^{(l-1)}(\mathbf{Z}) (\log f_t(\mathbf{Z}; \theta_t) + \log p_t) \right\}, \quad (7)$$

where $\hat{\delta}^{(l)}$ is the estimate of δ at the l th iteration. As a result of the iterative application of the E-step and M-step, we obtain a nondecreasing sequence of log-likelihood function values such that $\log f(\mathbf{Z}; \delta^{(l+1)}) > \log f(\mathbf{Z}; \delta^{(l)})$, and this procedure is repeated until a stopping criterion is not satisfied. The above cyclic procedures need an initial value for δ denoted by $\hat{\delta}^{(0)}$.

As a final remark, notice that the hidden (or missing) random variable c can be viewed as a random parameter with an *a priori* distribution given by p_t , $t = 0, 1$. Thus, problem (1) encompasses both deterministic and random parameters. This point is important to better frame the detector devised in the next subsection.

A. Detection Architecture Design

From the above procedures, it turns out that the E-steps iteratively update the estimates of *a posteriori* probabilities which can be used to evaluate the “responsibility” that the hypotheses take for “explaining” the data [56]. Specifically, let us consider the Bayesian framework² and if the all the parameters were known, the decision rule based upon the minimization of the Bayesian risk would be

$$\frac{p_1 f_1(\mathbf{Z}; \theta_1)}{p_0 f_0(\mathbf{Z}; \theta_0)} \underset{H_0}{\underset{H_1}{\geq}} \frac{C_{10} - C_{00}}{C_{01} - C_{11}}, \quad (8)$$

where C_{ij} , $i = 0, 1$, $j = 0, 1$, is the cost for selecting H_i when H_j is true. However, assuming the perfect knowledge of the parameter values is not reasonable in practice and, hence, we replace them with estimates returned by the EM algorithm to come up with

$$\frac{\hat{p}_1^{(l_{\max})} f_1(\mathbf{Z}; \hat{\theta}_1^{(l_{\max})})}{\hat{p}_0^{(l_{\max})} f_0(\mathbf{Z}; \hat{\theta}_0^{(l_{\max})})} \underset{H_0}{\underset{H_1}{\geq}} \frac{C_{10} - C_{00}}{C_{01} - C_{11}}. \quad (9)$$

Thus, the considered framework jointly exploits the Bayesian and the ML approach [57]. Finally, the costs are used to tune P_{fa} , which is of primary concern in radar [58], by defining the following detection threshold

$$\eta = \frac{C_{10} - C_{00}}{C_{01} - C_{11}}. \quad (10)$$

The corresponding detection architecture becomes

$$\frac{\hat{p}_1^{(l_{\max})} f_1(\mathbf{Z}; \hat{\theta}_1^{(l_{\max})})}{\hat{p}_0^{(l_{\max})} f_0(\mathbf{Z}; \hat{\theta}_0^{(l_{\max})})} \underset{H_0}{\underset{H_1}{\geq}} \eta. \quad (11)$$

Three remarks are now in order. First, notice that η can be set according to the desired P_{fa} . Second, the left-hand

²Notice that we are implicitly treating c as a random parameter.

side of (11) shares a similar structure with the GLRT that, however, does not exploit any estimate of p_0 and p_1 . It is also important to highlight that (11) is statistically equivalent to

$$\frac{q_1^{(l_{\max})}(\mathbf{Z})}{q_0^{(l_{\max})}(\mathbf{Z})} \underset{H_0}{\underset{H_1}{\geq}} \eta, \quad (12)$$

that can be viewed as a “generalized MAP” detector. The word “generalized” is used to indicate that the above detector can be considered a modification of the MAP rule obtained by introducing η and by replacing the unknown parameters with ML-based estimates. In the following, this detector will be referred to as Joint Bayesian-ML Detector based on EM algorithm (EM-BML-D).

The final expression of (11) can be obtained by solving (7). To this end, let us observe that in (7), the optimization with respect to $\mathbf{p} = [p_0, p_1]^T$ and $\theta = [\theta_0^T, \theta_1^T]^T$ are independent. Thus, the estimates of \mathbf{p} and θ at the l th iteration can be separately obtained as

$$\hat{\theta}^{(l)} = \arg \max_{\theta} \left\{ q_0^{(l-1)}(\mathbf{Z}) \log f_0(\mathbf{Z}; \theta_0) + q_1^{(l-1)}(\mathbf{Z}) \log f_1(\mathbf{Z}; \theta_1) \right\} \quad (13a)$$

$$\hat{\mathbf{p}}^{(l)} = \arg \max_{\mathbf{p}} \sum_{t=0}^1 q_t^{(l-1)}(\mathbf{Z}) \log p_t. \quad (13b)$$

It can be shown that the estimates of p_0 and p_1 are given by

$$\begin{aligned} \hat{p}_0^{(l)} &= q_0^{(l-1)}(\mathbf{Z}), \\ \hat{p}_1^{(l)} &= q_1^{(l-1)}(\mathbf{Z}). \end{aligned} \quad (14)$$

Now, the optimization problem with respect to θ can be recast as

$$\begin{aligned} & \max_{\mathbf{M}, \alpha} \left\{ q_0^{(l-1)}(\mathbf{Z}) \log f_0(\mathbf{Z}; \theta_0) + q_1^{(l-1)}(\mathbf{Z}) \log f_1(\mathbf{Z}; \theta_1) \right\}, \\ & \Rightarrow \max_{\mathbf{M}, \alpha} \left\{ -(K+1) \log \det(\mathbf{M}) - \text{Tr} \left[\mathbf{M}^{-1} \left(q_0^{(l-1)}(\mathbf{Z}) \mathbf{Z} \mathbf{Z}^\dagger + q_1^{(l-1)}(\mathbf{Z}) \left((z - \alpha \mathbf{v})(z - \alpha \mathbf{v})^\dagger + \mathbf{S} \right) \right) \right] \right\}. \end{aligned} \quad (15)$$

Setting to zero the first derivative with respect to \mathbf{M} yields

$$\begin{aligned} & -(K+1)(\mathbf{M}^T)^{-1} + q_0^{(l-1)}(\mathbf{Z}) \left[(\mathbf{M}^T)^{-1} (\mathbf{Z} \mathbf{Z}^\dagger)^T (\mathbf{M}^T)^{-1} \right] \\ & + q_1^{(l-1)}(\mathbf{Z}) \left[(\mathbf{M}^T)^{-1} \left((z - \alpha \mathbf{v})(z - \alpha \mathbf{v})^\dagger + \mathbf{S} \right)^T (\mathbf{M}^T)^{-1} \right] \\ & = \mathbf{0}. \end{aligned} \quad (16)$$

Thus, the estimate of \mathbf{M} at the l th M-step is given by

$$\begin{aligned} \hat{\mathbf{M}}^{(l)} &= \frac{1}{K+1} \left[q_0^{(l-1)}(\mathbf{Z}) \mathbf{Z} \mathbf{Z}^\dagger + q_1^{(l-1)}(\mathbf{Z}) \left((z - \alpha \mathbf{v})(z - \alpha \mathbf{v})^\dagger + \mathbf{S} \right) \right]. \end{aligned} \quad (17)$$

Plugging (17) into (15) leads to

$$\begin{aligned}
& \max_{\alpha} -(K+1) \log \det(\widehat{\mathbf{M}}_{(l)}) \\
\Rightarrow & \min_{\alpha} \log \det \left\{ q_0^{(l-1)}(\mathbf{Z}) \mathbf{Z} \mathbf{Z}^\dagger \right. \\
& \quad \left. + q_1^{(l-1)}(\mathbf{Z}) [(z - \alpha \mathbf{v})(z - \alpha \mathbf{v})^\dagger + \mathbf{S}] \right\} \\
\Rightarrow & \min_{\alpha} \log \det \left\{ \mathbf{A}_{(l)} + q_1^{(l-1)}(\mathbf{Z}) (z - \alpha \mathbf{v})(z - \alpha \mathbf{v})^\dagger \right\},
\end{aligned} \tag{18}$$

where $\mathbf{A}_{(l)} = q_0^{(l-1)}(\mathbf{Z}) \mathbf{Z} \mathbf{Z}^\dagger + q_1^{(l-1)}(\mathbf{Z}) \mathbf{S}$. The determinant in (18) can be further written as

$$\begin{aligned}
& \det \left\{ \mathbf{A}_{(l)} + q_1^{(l-1)}(\mathbf{Z}) (z - \alpha \mathbf{v})(z - \alpha \mathbf{v})^\dagger \right\} \\
& = \det(\mathbf{A}_{(l)}) \left[1 + q_1^{(l-1)}(\mathbf{Z}) (z - \alpha \mathbf{v})^\dagger \mathbf{A}_{(l)}^{-1} (z - \alpha \mathbf{v}) \right].
\end{aligned} \tag{19}$$

Setting to zero the first derivative of the objective function with respect to α leads to

$$\widehat{\alpha}^{(l)} = \frac{\mathbf{v}^\dagger \mathbf{A}_{(l)}^{-1} z}{\mathbf{v}^\dagger \mathbf{A}_{(l)}^{-1} \mathbf{v}}. \tag{20}$$

After l_{\max} iterations, plugging the above estimates into (11), the EM-BML-D can be finally written as

$$\begin{aligned}
& \frac{\widehat{p}_1^{(l_{\max})}}{\widehat{p}_0^{(l_{\max})}} \exp \left\{ z^\dagger \widehat{\mathbf{M}}_{(l_{\max})}^{-1} z \right. \\
& \quad \left. - (z - \widehat{\alpha}^{(l_{\max})} \mathbf{v})^\dagger \widehat{\mathbf{M}}_{(l_{\max})}^{-1} (z - \widehat{\alpha}^{(l_{\max})} \mathbf{v}) \right\} \underset{H_0}{\overset{H_1}{\geq}} \eta.
\end{aligned} \tag{21}$$

In next section, we focus on the CFAR property of (21) with respect to M , and show that the test statistic of EM-BML-D is invariant with respect to the interference covariance matrix under a specific initialization.

III. CFAR properties

Since the decision statistic in (11) depends on the iteration index l , we resort to the mathematical induction to prove the following proposition.

PROPOSITION 1 $\frac{q_1^{(l)}(\mathbf{Z})}{q_0^{(l)}(\mathbf{Z})}$ is CFAR with respect to M provided that the distribution of $\frac{q_1^{(l-1)}(\mathbf{Z})}{q_0^{(l-1)}(\mathbf{Z})}$ is invariant with respect to M .

Proof:

Let us start by observing that from (14), when the distribution of $\frac{q_1^{(l-1)}(\mathbf{Z})}{q_0^{(l-1)}(\mathbf{Z})}$ does not depend on M , then also that of $\frac{\widehat{p}_1^{(l)}}{\widehat{p}_0^{(l)}}$ exhibits this property. Furthermore, notice

that³

$$\begin{aligned}
q_0^{(l-1)}(\mathbf{Z}) & = \frac{\widehat{p}_0^{(l-1)} f_0(\mathbf{Z}; \widehat{\boldsymbol{\theta}}_0^{(l-1)})}{\widehat{p}_0^{(l-1)} f_0(\mathbf{Z}; \widehat{\boldsymbol{\theta}}_0^{(l-1)}) + \widehat{p}_1^{(l-1)} f_1(\mathbf{Z}; \widehat{\boldsymbol{\theta}}_1^{(l-1)})} \\
& = \frac{1}{1 + \frac{\widehat{p}_1^{(l-1)} f_1(\mathbf{Z}; \widehat{\boldsymbol{\theta}}_1^{(l-1)})}{\widehat{p}_0^{(l-1)} f_0(\mathbf{Z}; \widehat{\boldsymbol{\theta}}_0^{(l-1)})}} \\
& = \frac{1}{1 + \frac{q_1^{(l-1)}(\mathbf{Z})}{q_0^{(l-1)}(\mathbf{Z})}}.
\end{aligned} \tag{22}$$

Therefore, the distribution of $q_0^{(l-1)}(\mathbf{Z})$ is independent of M . The same line of reasoning can be applied to show that $q_1^{(l-1)}(\mathbf{Z})$ has a distribution independent of M .

From (21), let us define

$$g(\widehat{\boldsymbol{\theta}}_0^{(l)}, \widehat{\boldsymbol{\theta}}_1^{(l)}; \mathbf{Z}) = z^\dagger \widehat{\mathbf{M}}_{(l)}^{-1} z - (z - \widehat{\alpha}^{(l)} \mathbf{v})^\dagger \widehat{\mathbf{M}}_{(l)}^{-1} (z - \widehat{\alpha}^{(l)} \mathbf{v}), \tag{23}$$

which can be written as

$$\begin{aligned}
& g(\widehat{\boldsymbol{\theta}}_0^{(l)}, \widehat{\boldsymbol{\theta}}_1^{(l)}; \mathbf{Z}) \\
& = z^\dagger \widehat{\mathbf{M}}_{(l)}^{-1} z - z^\dagger \widehat{\mathbf{M}}_{(l)}^{-1} z + (\widehat{\alpha}^{(l)})^\dagger \mathbf{v}^\dagger \widehat{\mathbf{M}}_{(l)}^{-1} z \\
& \quad + \widehat{\alpha}^{(l)} z^\dagger \widehat{\mathbf{M}}_{(l)}^{-1} \mathbf{v} - |\widehat{\alpha}^{(l)}|^2 \mathbf{v}^\dagger \widehat{\mathbf{M}}_{(l)}^{-1} \mathbf{v} \\
& = \frac{z^\dagger \mathbf{A}_{(l)}^{-1} \mathbf{v} \mathbf{v}^\dagger \widehat{\mathbf{M}}_{(l)}^{-1} z}{\mathbf{v}^\dagger \mathbf{A}_{(l)}^{-1} \mathbf{v}} + \frac{\mathbf{v}^\dagger \mathbf{A}_{(l)}^{-1} z z^\dagger \widehat{\mathbf{M}}_{(l)}^{-1} \mathbf{v}}{\mathbf{v}^\dagger \mathbf{A}_{(l)}^{-1} \mathbf{v}} \\
& \quad - \frac{\mathbf{v}^\dagger \mathbf{A}_{(l)}^{-1} z z^\dagger \mathbf{A}_{(l)}^{-1} \mathbf{v} \mathbf{v}^\dagger \widehat{\mathbf{M}}_{(l)}^{-1} \mathbf{v}}{(\mathbf{v}^\dagger \mathbf{A}_{(l)}^{-1} \mathbf{v})^2}.
\end{aligned} \tag{24}$$

Let $\bar{\mathbf{v}} = M^{-\frac{1}{2}} \mathbf{v}$ and $\bar{\mathbf{z}} = M^{-\frac{1}{2}} z$, then we have

$$\begin{aligned}
& g(\widehat{\boldsymbol{\theta}}_0^{(l)}, \widehat{\boldsymbol{\theta}}_1^{(l)}; \mathbf{Z}) \\
& = \frac{\bar{\mathbf{z}}^\dagger M^{\frac{1}{2}} \mathbf{A}_{(l)}^{-1} M^{\frac{1}{2}} \bar{\mathbf{v}} \bar{\mathbf{v}}^\dagger M^{\frac{1}{2}} \widehat{\mathbf{M}}_{(l)}^{-1} M^{\frac{1}{2}} \bar{\mathbf{z}}}{\bar{\mathbf{v}}^\dagger M^{\frac{1}{2}} \mathbf{A}_{(l)}^{-1} M^{\frac{1}{2}} \bar{\mathbf{v}}} \\
& \quad + \frac{\bar{\mathbf{v}}^\dagger M^{\frac{1}{2}} \mathbf{A}_{(l)}^{-1} M^{\frac{1}{2}} \bar{\mathbf{z}} \bar{\mathbf{z}}^\dagger M^{\frac{1}{2}} \widehat{\mathbf{M}}_{(l)}^{-1} M^{\frac{1}{2}} \bar{\mathbf{v}}}{\bar{\mathbf{v}}^\dagger M^{\frac{1}{2}} \mathbf{A}_{(l)}^{-1} M^{\frac{1}{2}} \bar{\mathbf{v}}} \\
& \quad - \frac{\bar{\mathbf{v}}^\dagger M^{\frac{1}{2}} \mathbf{A}_{(l)}^{-1} M^{\frac{1}{2}} \bar{\mathbf{z}} \bar{\mathbf{z}}^\dagger M^{\frac{1}{2}} \mathbf{A}_{(l)}^{-1} M^{\frac{1}{2}} \bar{\mathbf{v}} \bar{\mathbf{v}}^\dagger M^{\frac{1}{2}} \widehat{\mathbf{M}}_{(l)}^{-1} M^{\frac{1}{2}} \bar{\mathbf{v}}}{(\bar{\mathbf{v}}^\dagger M^{\frac{1}{2}} \mathbf{A}_{(l)}^{-1} M^{\frac{1}{2}} \bar{\mathbf{v}})^2} \\
& = \frac{\bar{\mathbf{z}}^\dagger \bar{\mathbf{A}}_{(l)}^{-1} \bar{\mathbf{v}} \bar{\mathbf{v}}^\dagger \bar{\mathbf{M}}_{(l)}^{-1} \bar{\mathbf{z}}}{\bar{\mathbf{v}}^\dagger \bar{\mathbf{A}}_{(l)}^{-1} \bar{\mathbf{v}}} + \frac{\bar{\mathbf{v}}^\dagger \bar{\mathbf{A}}_{(l)}^{-1} \bar{\mathbf{z}} \bar{\mathbf{z}}^\dagger \bar{\mathbf{M}}_{(l)}^{-1} \bar{\mathbf{v}}}{\bar{\mathbf{v}}^\dagger \bar{\mathbf{A}}_{(l)}^{-1} \bar{\mathbf{v}}} \\
& \quad - \frac{\bar{\mathbf{v}}^\dagger \bar{\mathbf{A}}_{(l)}^{-1} \bar{\mathbf{z}} \bar{\mathbf{z}}^\dagger \bar{\mathbf{A}}_{(l)}^{-1} \bar{\mathbf{v}} \bar{\mathbf{v}}^\dagger \bar{\mathbf{M}}_{(l)}^{-1} \bar{\mathbf{v}}}{(\bar{\mathbf{v}}^\dagger \bar{\mathbf{A}}_{(l)}^{-1} \bar{\mathbf{v}})^2},
\end{aligned} \tag{25}$$

where

$$\begin{aligned}
\bar{\mathbf{A}}_{(l)} & = M^{-\frac{1}{2}} \mathbf{A}_{(l)} M^{-\frac{1}{2}} \\
& = q_0^{(l-1)}(\mathbf{Z}) M^{-\frac{1}{2}} \mathbf{Z} \mathbf{Z}^\dagger M^{-\frac{1}{2}} + q_1^{(l-1)}(\mathbf{Z}) M^{-\frac{1}{2}} \mathbf{S} M^{-\frac{1}{2}}
\end{aligned} \tag{26}$$

³Notice that we do not consider the case that \widehat{p}_0 , \widehat{p}_1 , q_0 , or $q_1 = 0$.

$$\begin{aligned}
\bar{M}_{(l)} &= M^{-\frac{1}{2}} \widehat{M}_{(l)} M^{-\frac{1}{2}} \\
&= \frac{1}{K+1} \left[q_0^{(l-1)}(\mathbf{Z}) M^{-\frac{1}{2}} \mathbf{Z} \mathbf{Z}^\dagger M^{-\frac{1}{2}} + \right. \\
&\quad \left. q_1^{(l-1)}(\mathbf{Z}) \left(M^{-\frac{1}{2}} (\mathbf{z} - \widehat{\alpha}^{(l)} \mathbf{v}) (\mathbf{z} - \widehat{\alpha}^{(l)} \mathbf{v})^\dagger M^{-\frac{1}{2}} + \right. \right. \\
&\quad \left. \left. M^{-\frac{1}{2}} \mathbf{S} M^{-\frac{1}{2}} \right) \right] \\
&= \frac{1}{K+1} \left[\bar{\mathbf{A}}_{(l)} + q_1^{(l-1)}(\mathbf{Z}) (\bar{\mathbf{z}} - \widehat{\alpha}^{(l)} \bar{\mathbf{v}}) (\bar{\mathbf{z}} - \widehat{\alpha}^{(l)} \bar{\mathbf{v}})^\dagger \right]
\end{aligned} \tag{27}$$

Since $M^{-\frac{1}{2}} \mathbf{Z} \mathbf{Z}^\dagger M^{-\frac{1}{2}} \sim \mathcal{CW}(K+1, N; \mathbf{I}_N)$ and $M^{-\frac{1}{2}} \mathbf{S} M^{-\frac{1}{2}} \sim \mathcal{CW}(K, N; \mathbf{I}_N)$, it follows that $\bar{\mathbf{A}}_{(l)}$ is invariant to the interference covariance matrix M .

Now, we introduce a unitary transformation that rotates the whitened steering vector into the first elementary vector

$$\mathbf{U}^\dagger \bar{\mathbf{v}} = \sqrt{\mathbf{v}^\dagger M^{-1} \mathbf{v}} \mathbf{e}_1, \tag{28}$$

where $\mathbf{U} \in \mathbb{C}^{N \times N}$ is a unitary matrix and $\mathbf{e}_1 = [1, 0, \dots, 0]^T \in \mathbb{C}^{N \times 1}$. Then $g(\widehat{\theta}_0^{(l)}, \widehat{\theta}_1^{(l)}; \mathbf{Z})$ can be recast as

$$\begin{aligned}
g(\widehat{\theta}_0^{(l)}, \widehat{\theta}_1^{(l)}; \mathbf{Z}) &= \frac{\bar{\mathbf{z}}^\dagger \bar{\mathbf{A}}_{(l)}^{-1} \mathbf{e}_1 \mathbf{e}_1^\dagger \bar{M}_{(l)}^{-1} \bar{\mathbf{z}}}{\mathbf{e}_1^\dagger \bar{\mathbf{A}}_{(l)}^{-1} \mathbf{e}_1} + \frac{\mathbf{e}_1^\dagger \bar{\mathbf{A}}_{(l)}^{-1} \bar{\mathbf{z}} \bar{\mathbf{z}}^\dagger \bar{M}_{(l)}^{-1} \mathbf{e}_1}{\mathbf{e}_1^\dagger \bar{\mathbf{A}}_{(l)}^{-1} \mathbf{e}_1} \\
&\quad - \frac{\mathbf{e}_1^\dagger \bar{\mathbf{A}}_{(l)}^{-1} \bar{\mathbf{z}} \bar{\mathbf{z}}^\dagger \bar{\mathbf{A}}_{(l)}^{-1} \mathbf{e}_1 \mathbf{e}_1^\dagger \bar{M}_{(l)}^{-1} \mathbf{e}_1}{(\mathbf{e}_1^\dagger \bar{\mathbf{A}}_{(l)}^{-1} \mathbf{e}_1)^2}, \tag{29}
\end{aligned}$$

where

$$\begin{cases} \bar{\mathbf{z}} &= \mathbf{U}^\dagger \mathbf{z} \sim \mathcal{CN}(0, \mathbf{I}_N), \\ \bar{\mathbf{A}}_{(l)} &= \mathbf{U}^\dagger \bar{\mathbf{A}}_{(l)} \mathbf{U} \text{ obeys the same distribution as } \bar{\mathbf{A}}_{(l)}, \\ \bar{M}_{(l)} &= \mathbf{U}^\dagger M_{(l)} \mathbf{U} \\ &\propto \left[\bar{\mathbf{A}}_{(l)} + q_1^{(l-1)}(\mathbf{Z}) (\bar{\mathbf{z}} - \widehat{\alpha}_w^{(l)} \mathbf{e}_1) (\bar{\mathbf{z}} - \widehat{\alpha}_w^{(l)} \mathbf{e}_1)^\dagger \right] \end{cases} \tag{30}$$

$$\text{with } \widehat{\alpha}_w^{(l)} = \sqrt{\mathbf{v}^\dagger M^{-1} \mathbf{v}} \widehat{\alpha}^{(l)} = \frac{\mathbf{e}_1^\dagger \bar{\mathbf{A}}_{(l)}^{-1} \bar{\mathbf{z}}}{\mathbf{e}_1^\dagger \bar{\mathbf{A}}_{(l)}^{-1} \mathbf{e}_1}.$$

With all of the results above, it can be seen that when $\frac{q_1^{(l-1)}(\mathbf{Z})}{q_0^{(l-1)}(\mathbf{Z})}$ is CFAR with respect to M , $\frac{q_1^{(l)}(\mathbf{Z})}{q_0^{(l)}(\mathbf{Z})}$ includes no real interference covariance M in the statistical characteristic, and thus ensures the CFAR property. ■

Gathering the above results, it turns out that when $\frac{q_1^{(0)}(\mathbf{Z})}{q_0^{(0)}(\mathbf{Z})}$ is independent of M , we can claim that for a given l_{\max} , the EM-BML-D proposed in (21) possesses the CFAR with respect to M .

IV. Performance Assessment

In this section, we assess the performance of the EM-BML-D in comparison with well-known competitors such as Kelly's GLRT, the AMF, Rao, and the ACE [59], [60]. At the same time, in order to learn the performance degradation of the proposed algorithm due to parameter estimation, we consider the test given by (11) with all parameters known (except for p_0 and p_1) as a benchmark. This detector is referred to in the ensuing numerical examples as "Benchmark". To this end, we resort to the Monte Carlo counting techniques and obtain the detection threshold corresponding to a pre-assigned P_{fa} through

$100/P_{fa}$ independent trials, and the Probability of Detection (P_d) through 1000 independent trials, respectively.

Specifically, we investigate the following aspects:

- 1) the convergence rate of the cyclic procedure based upon the EM algorithm;
- 2) the CFAR behavior of the EM-BML-D with respect to the disturbance covariance matrix;
- 3) the detection performance in the presence of perfectly matched signals under different configurations;
- 4) the rejection capability of mismatched target echoes.

A. Initialization Issues and Simulation Setup

In the next illustrative examples, we assume that the interference covariance matrix is $M = \sigma^2 \mathbf{I}_N + \sigma_c^2 M_c$, where $\sigma^2 \mathbf{I}_N$ is the thermal noise component with $\sigma^2 = 1$ the noise power and $\sigma_c^2 > 0$ is the clutter power set according to the Clutter-to-Noise-Ratio (CNR) given by $\text{CNR} = 10 \log(\sigma_c^2/\sigma^2)$. As for the clutter covariance matrix M_c , we assume that its (i, j) th entry is equal to $\rho^{|i-j|}$ with $\rho = 0.9$ the one-lag correlation coefficient. Moreover, we define the Signal-to-Clutter-plus-Noise-Ratio (SCNR)

$$\text{SCNR} = |\alpha|^2 \mathbf{v}_t^\dagger M^{-1} \mathbf{v}_t, \tag{31}$$

where \mathbf{v}_t is the true target steering vector that is equal to the nominal steering vector \mathbf{v} in a perfectly matched scenario.

For initialization purpose, we set $\widehat{p}_0^{(0)} = \widehat{p}_1^{(0)} = 1/2$, while $\widehat{M}_{(0)}$ is equal to \mathbf{S} . As for the initial value of $\widehat{\alpha}^{(0)}$, a reasonable choice is

$$\widehat{\alpha}^{(0)} = \frac{\mathbf{v}^\dagger \mathbf{S}^{-1} \mathbf{z}}{\mathbf{v}^\dagger \mathbf{S}^{-1} \mathbf{v}}. \tag{32}$$

It is important to underline that with this initializations, $\frac{q_1^{(0)}(\mathbf{Z})}{q_0^{(0)}(\mathbf{Z})}$ can be written as

$$\begin{aligned}
\frac{q_1^{(0)}(\mathbf{Z})}{q_0^{(0)}(\mathbf{Z})} &= \frac{\widehat{p}_0^{(0)}}{\widehat{p}_1^{(0)}} \exp \left\{ g(\widehat{\alpha}^{(0)}, \mathbf{S}; \mathbf{Z}) \right\} \\
&= \frac{|\mathbf{v}^\dagger \mathbf{S}^{-1} \mathbf{z}|^2}{\mathbf{v}^\dagger \mathbf{S}^{-1} \mathbf{v}} = \frac{|\mathbf{e}_1^\dagger \bar{\mathbf{S}}^{-1} \bar{\mathbf{z}}|^2}{\mathbf{e}_1^\dagger \bar{\mathbf{S}}^{-1} \mathbf{e}_1}, \tag{33}
\end{aligned}$$

where $\bar{\mathbf{S}} = \mathbf{U}^\dagger M^{-\frac{1}{2}} \mathbf{S} M^{-\frac{1}{2}} \mathbf{U} \sim \mathcal{CW}(K, N; \mathbf{I}_N)$ indicates that $\frac{q_1^{(0)}(\mathbf{Z})}{q_0^{(0)}(\mathbf{Z})}$ is CFAR with respect to M .

B. The Convergence of the Cyclic Procedure

In this subsection, we investigate the convergence rate of the iterative estimation procedure. To this end, let $\mathcal{L}(\mathbf{Z}; \boldsymbol{\theta})$ be the objective function in (15), then the relative variation of the likelihood function due to the estimation of $\boldsymbol{\theta}$ at the l th iteration is defined as

$$\Delta \mathcal{L}(l) = \left| \frac{\mathcal{L}(\mathbf{Z}; \widehat{\boldsymbol{\theta}}^{(l)}) - \mathcal{L}(\mathbf{Z}; \widehat{\boldsymbol{\theta}}^{(l-1)})}{\mathcal{L}(\mathbf{Z}; \widehat{\boldsymbol{\theta}}^{(l)})} \right|. \tag{34}$$

Fig. 1 shows $\Delta\mathcal{L}(l)$ versus l under H_0 averaged over 1000 independent Monte Carlo trials for different configurations of N and K . As it is observed, the curves rapidly decrease as l increases and for high values of N and K , the variation further decreases due to the increased estimation quality. More importantly, for the considered cases under H_0 , the average relative variation is lower than 10^{-4} for $l \geq 4$ and reduces to 10^{-5} at $l = 6$. Such a behavior are confirmed in Fig. 2 which corresponds to H_1 and contains the curves of $\Delta\mathcal{L}(l)$ for different SCNR values. Specifically, the variation is lower than 10^{-5} when $l \geq 5$. Finally, notice that for a given configuration, the variation significantly reduces when the SCNR increases.

Summarizing, as a compromise between the computational burden and the optimization performance, we use $l_{\max} = 5$ in the ensuing simulations. For the sake of comparison, we also consider $l_{\max} = 7$.

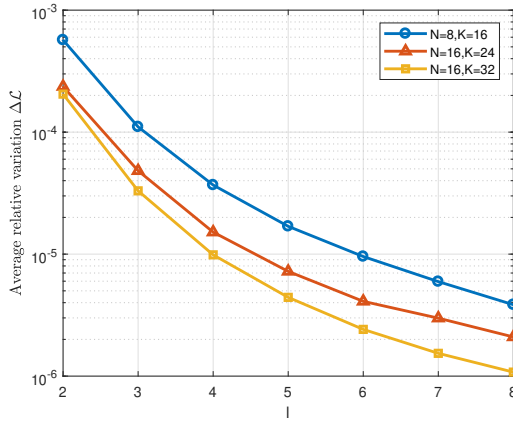


Fig. 1: $\Delta\mathcal{L}(l)$ versus iteration number under H_0 , $\rho = 0.9$, CNR= 30 dB.

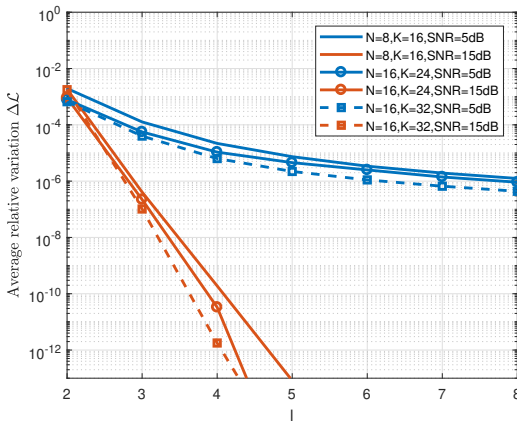


Fig. 2: $\Delta\mathcal{L}(l)$ versus iteration number under H_1 , $\rho = 0.9$, CNR= 30 dB.

C. The CFAR Properties

Let us recall that in Section III, we proved the CFAR property of the EM-BML-D with respect to the statistical properties of the disturbance. In this subsection, we corroborate the results presented in Section III by resorting to Monte Carlo simulation. For completeness, we also consider the aforementioned competitors. In, Fig. 3 and Fig. 4, we use thresholds corresponding to a nominal $P_{fa} = 10^{-4}$ with $N = 8$, $K = 16$, $\rho = 0.9$, and CNR= 30 dB to evaluate the actual P_{fa} under different CNR and ρ values. In the figures, EM-BML-D5 and EM-BML-D7 stand for the EM-BML-D with $l_{\max} = 5$ and $l_{\max} = 7$, respectively. It can be seen from the figures that the EM-BML-D is capable of maintaining the pre-assigned P_{fa} when the CNR varies from 30 dB to 110 dB and ρ changes from 0.5 to 0.9.

Such a corroboration of the CFAR property can also be observed under other configurations of N and K , and thus omitted here for brevity.

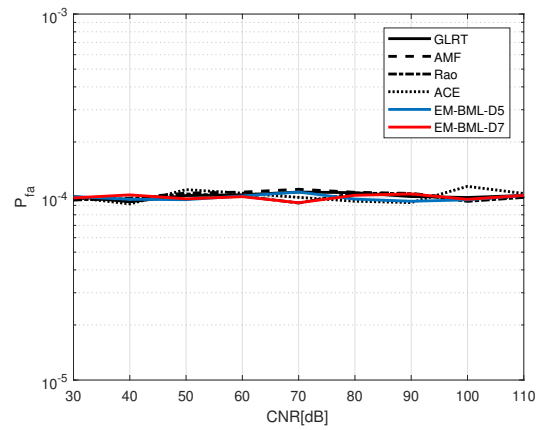


Fig. 3: P_{fa} versus CNR, assuming $N = 8$, $K = 16$, $\rho = 0.9$, nominal CNR= 30 dB.

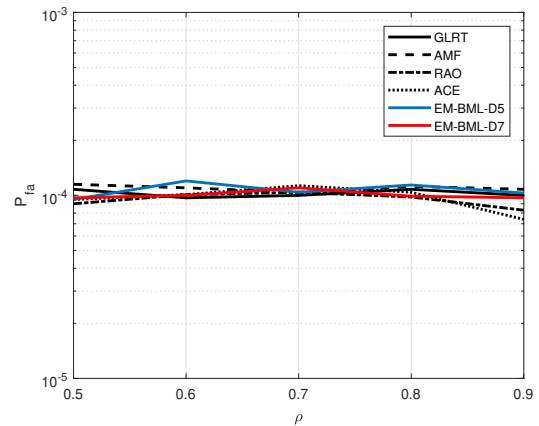


Fig. 4: P_{fa} versus ρ , assuming $N = 8$, $K = 16$, CNR= 30 dB, nominal $\rho = 0.9$.

D. Matched Targets

The detection performance analysis starts from the case where the nominal steering vector \mathbf{v} and the actual steering vector \mathbf{v}_t are perfectly aligned or at least the misalignment is negligible. Moreover, we initially set $K = 2N$, which allows us to limit the detection loss related to the estimation of the interference parameters as claimed in [18], then we consider the so-called *sample-starved* scenario [8] where $N < K < 2N$.

Fig. 5 shows the P_d curves assuming $N = 8$, $K = 16$, and highlights that at least for the considered operating scenario, the proposed MAP-based detectors significantly outperform their conventional counterparts. To be more specific, it can be seen that the EM-BML-D5 and EM-BML-D7 ensure the best performance with $P_d > 0.8$ when SCNR = 15 dB, whereas the GLRT and AMF experience a P_d around 0.6 and 0.5, respectively. The performance enhancement is due to the fact that the information of both hypotheses has been combined through the latent variables to come up with the model of the received data, as shown in (4). Such a combination allows us to account for the hypothesis priors in the decision and estimation process. As a matter of fact, the estimates of the unknowns are linear combinations of H_0 and H_1 , with *a posteriori* probabilities as the coefficients (see (17) and (20)). At the same time, the EM algorithm endows the detection system with the capability of estimating the posterior information from data. Notice also that in Fig. 5, the EM-BML-D with $l_{\max} = 5$ and $l_{\max} = 7$ share almost the same performance, which may be due to the sufficiently small residual error of the cyclic procedure. In Table I, we report the execution time (averaged over 1000 Monte Carlo trials) for each of the considered detectors to provide an estimate of the respective computational complexity. Inspection of Table I points out that the EM-BML-D achieves better detection performance at the price of an increased computational burden (about one order of magnitude with respect to the competitors) due to the iterative estimation procedures. As expected, the EM-BML-D7 is more time-consuming than the EM-BML-D5. Similar results have been obtained under different parameter configurations and are not reported here for brevity.

TABLE I: Average Execution Times over 1000 Monte Carlo Trails

Detector	GLRT	AMF	Rao
Time(s)	2.29×10^{-5}	1.93×10^{-5}	2.30×10^{-5}
Detector	ACE	EM-BML-D5	EM-BML-D7
Time(s)	2.21×10^{-5}	3.81×10^{-4}	5.37×10^{-4}

To further corroborate the results observed in Fig. 5, in Fig. 6 we show the detection performance of the detectors assuming a parameter setting equal to that of Fig. 5, except for the values of N and K . It can be seen that the

EM-BML-D5 shares the same performance as EM-BML-D7 and ensures the highest performance in both figures. Notice that when $N = 16$, $K = 32$, the improvement of the EM-BML-D with respect to the counterparts decreases since the quality of covariance matrix estimates of the latter improves. From Fig. 6(b), it turns out that even though N and K become larger compared to Fig. 5, the detection performance may deteriorate due to the decrease of the ratio K/N . Finally, Fig. 7 shows the P_d curves of EM-BML-D5 and GLRT when $N = 16$ and K as a parameter. It can be observed that EM-BML-D5 with $K = 28$ outperforms the GLRT with $K = 32$.

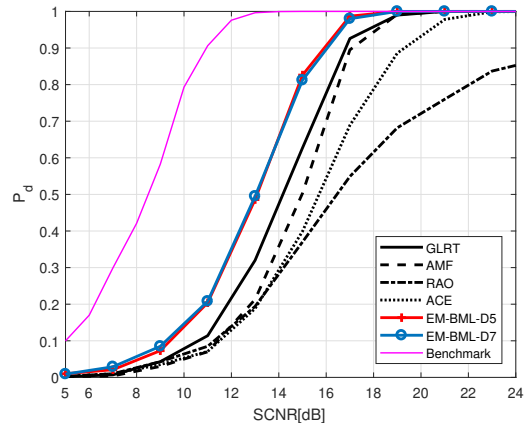
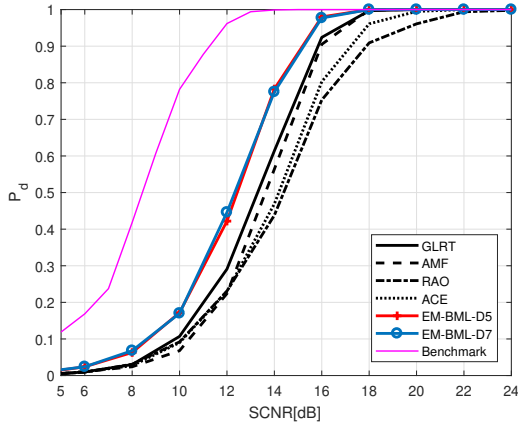


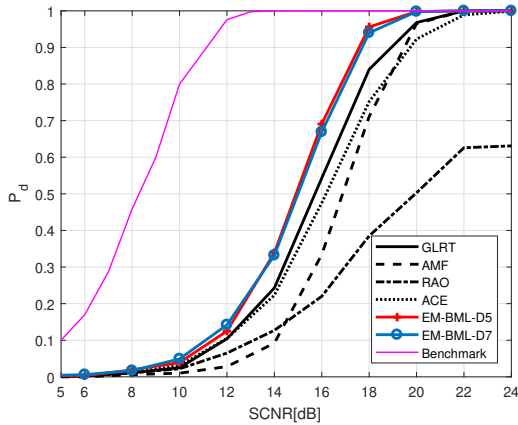
Fig. 5: P_d versus SCNR for matched targets, $N = 8$, $K = 16$, CNR = 30 dB.

To conclude this subsection, we assess the detection performance of the EM-BML-D5 using the real radar data collected by the MIT Lincoln Laboratory Phase One radar in 1985. The considered data set is *H067037.3* which contains 30 720 temporal returns and 76 range bins of L-band land clutter data with HH polarization. More details about the Phase One radar can be found in [1] and [61]. Analyses in [55] and [54] show that such data does not match the underlying assumption upon which the EM-BML-D is derived, namely homogeneous environment, and thus allows for an evaluation of the capability of adapting to different radar operating scenarios. Assuming $N = 8$ and $K = 16$, the threshold is first computed by considering range bin 28 as the CUT, and $K/2$ bins on each side of the CUT as secondary data, respectively, and we use 5 pulses of overlap in consecutive trials to achieve a sufficient number of Monte Carlo trials, namely $100/P_{fa}$ with $P_{fa} = 10^{-2}$. Before evaluating P_d , we estimate the P_{fa} of such a threshold on range bin 28 and 66, respectively, as shown in Table II and III. It can be seen that the threshold obtained on range bin 28 can maintain the desired P_{fa} also on bin 66 which is actually located in a nonhomogeneous region (see [55]).

As for the targets, they are injected into the CUT as done for synthetic data according to the SCNR defined in (31). Fig. 8 reports P_d of the detectors versus SCNR for range bin 28. It turns out that the EM-BML-D5



(a) $N = 16, K = 32$



(b) $N = 16, K = 24$

Fig. 6: P_d versus SCNR for matched targets, CNR = 30 dB.

TABLE II: Estimated P_{fa} for range bin 28 ($\times 10^{-2}$)

GLRT	AMF	Rao	ACE	EM-BML-D5
1.01	1.00	0.99	0.99	1.00

maintains a superior performance with respect to the counterparts confirming what have been observed in the case of synthetic data. Finally, we plot the curves of P_d versus SCNR using the same thresholds as in Fig. 8 with range bin 66 as the primary data, bins 57-64 and 68-75 as secondary data, in Fig. 9. Joint inspection of Table III and Fig. 9 indicates that the EM-BML-D5 enjoys a good capability of maintaining the P_{fa} constant in different regions and can overcome the competitors in terms of P_d .

E. Mismatched Targets

The analysis presented in this subsection considers the case where a mismatch between the true target steering vector \mathbf{v}_t and the nominal one exists. This analysis allows us to understand if the proposed detector is selective or

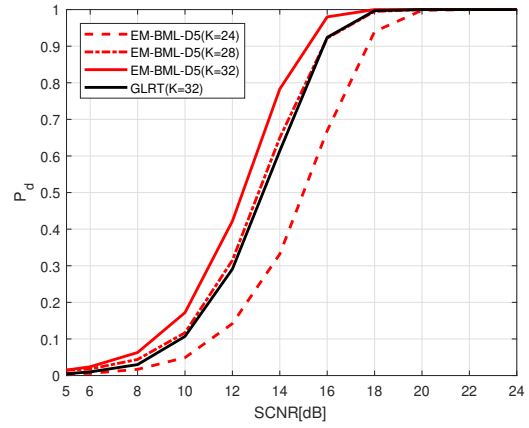


Fig. 7: P_d versus SCNR for matched targets, $N = 16$, CNR = 30 dB.

TABLE III: Estimated P_{fa} for range bin 66 ($\times 10^{-2}$)

GLRT	AMF	Rao	ACE	EM-BML-D5
1.19	1.7	1.3	1.3	1.23

robust [29]. Let us recall here that a selective detector rejects slightly mismatched signals with high probability whereas a robust detector is capable of guaranteeing high detection probabilities in the presence of uncertainties in the nominal steering vector. To this end, we evaluate the rejection capability of the detectors in terms of the mismatch angle ϕ defined as

$$\cos^2 \phi = \frac{|\mathbf{v}^\dagger \mathbf{M}^{-1} \mathbf{v}_t|^2}{(\mathbf{v}^\dagger \mathbf{M}^{-1} \mathbf{v})(\mathbf{v}_t^\dagger \mathbf{M}^{-1} \mathbf{v}_t)}. \quad (35)$$

Observe that in (35), $\cos^2 \phi = 1$ represents the perfectly matched case addressed in the previous subsection, whereas $\cos^2 \phi = 0$ corresponds to the totally mismatched scenario, namely \mathbf{v}_t is orthogonal to \mathbf{v} in the whitened observation space.

Fig. 10 contains the contours of constant P_d as a function of the $\cos^2 \phi$ and SCNR. Inspection of the figure shows that the EM-BML-D proposed in this paper exhibits a similar performance in terms of rejection capability of mismatched targets as the AMF. In fact, in the low SCNR region, the EM-BML-D exhibits the lowest selectivity. In the high SCNR region, the EM-BML-D rejects mismatched signals slightly better than the AMF. Otherwise stated, the EM-BML-D is the most robust detector in the presence of target mismatch. In Fig. 11, we analyze the performance in the case of mismatched signals from another perspective by plotting the curves of P_d versus $\cos^2 \phi$ for a given value of SCNR such that all of the detectors exhibit $P_d = 1$ at $\cos^2 \phi = 1$ (except for Rao test). In fact, the P_d of Rao test in Fig. 11(a) is 0 when $\cos^2 \phi < 0.9$ and equals to 0.84 at $\cos^2 \phi = 1$. Notice that Fig. 11 is actually a slice of Fig. 10 at SCNR = 25 dB. From the inspection of the figure, it turns out that the EM-BML-D has a robustness that is similar to

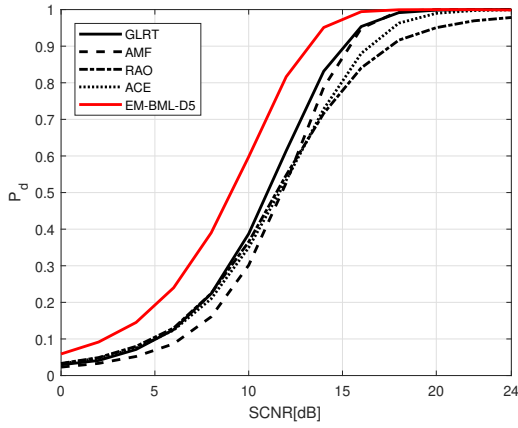


Fig. 8: P_d versus SCNR for real recorded data, range bin 28 used for both threshold estimation and P_d evaluation, $l_{\max} = 5$.

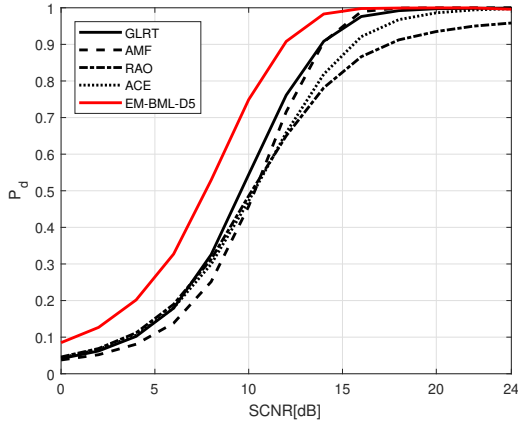
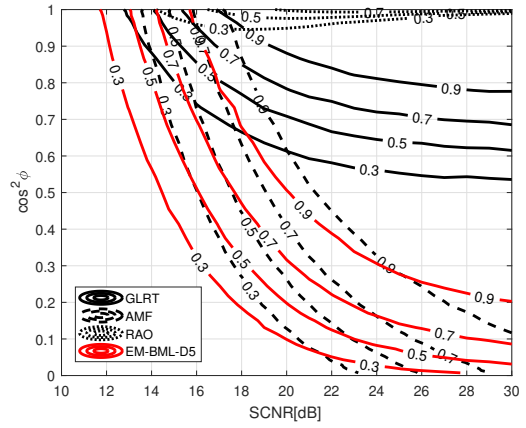


Fig. 9: P_d versus SCNR for real recorded data, range bin 28 used for threshold estimation, range bin 66 used for P_d evaluation, $l_{\max} = 5$.

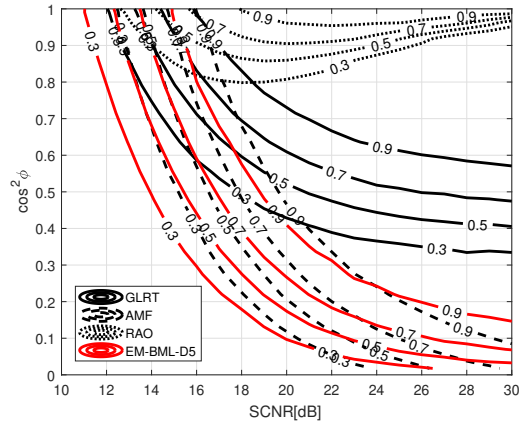
that of the AMF while is less selective than the GLRT and Rao.

V. Conclusion

In this paper, we have proposed a new radar target detection architecture grounded on the Bayesian framework and by exploiting the estimates from the EM algorithm in the presence of latent random variables. Precisely, the posterior information provided by the recursive procedure of the EM algorithm allows for the evaluation of the responsibility that the hypotheses take in “explaining” the data, and thus the decision for the presence of a potential target. At the design stage, we have modeled distribution of the collected data as a combination of the distributions under the two hypotheses, and we have used the estimates provided by the EM algorithm to build up a Bayesian detector. More importantly, we have proved that the proposed detector ensures the desired CFAR property



(a) $N = 8, K = 16$



(b) $N = 16, K = 32$

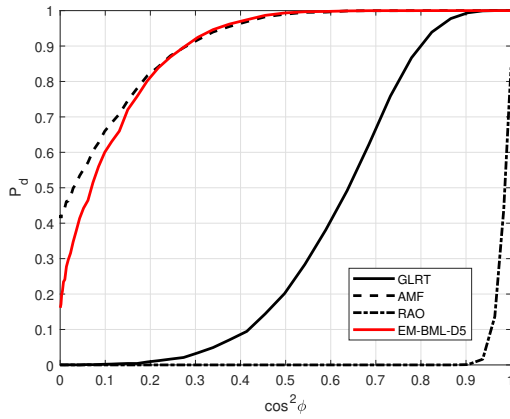
Fig. 10: Contours of constant P_d for mismatched targets, CNR = 30 dB.

with respect to the disturbance covariance matrix. The illustrative examples have shown that the proposed EM-BML-D significantly outperforms the considered conventional counterparts in terms of matched target detection and is robust to mismatched signals.

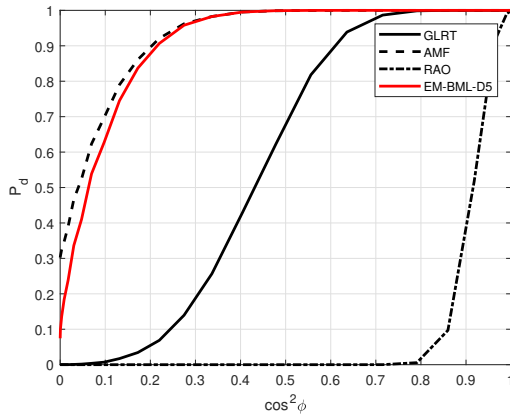
Future research tracks may encompass the design of selective schemes based on the EM algorithm and the Bayesian framework. The generalization of EM-BML-D towards multiple alternative hypothesis test also represents an interesting direction for the next works.

REFERENCES

- [1] C. Hao, D. Orlando, J. Liu, and C. Yin, *Advances in Adaptive Radar Detection and Range Estimation*, Springer, Ed., Singapore, 2022.
- [2] S. M. Kay, *Fundamentals of Statistical Signal Processing: Detection Theory*, P. Hall, Ed., 1998, vol. 2.
- [3] E. J. Kelly, “An adaptive detection algorithm,” *IEEE Transactions on Aerospace and Electronic Systems*, vol. 22, no. 1, pp. 115–127, 1986.
- [4] F. C. Robey, D. R. Fuhrmann, R. Nitzberg, and E. J. Kelly, “CFAR adaptive matched filter detector,” *IEEE Transactions on Aerospace and Electronic Systems*, vol. 28, no. 1, pp. 208–216, 1992.



(a) $N = 8, K = 16, \text{SCNR} = 25 \text{ dB}$



(b) $N = 16, K = 32, \text{SCNR} = 25 \text{ dB}$

Fig. 11: P_d versus $\cos^2\phi$ for constant SCNR, CNR = 30 dB.

[5] A. D. Maio, A. Farina, and G. Foglia, "Knowledge-aided Bayesian radar detectors & their application to live data," *IEEE Transactions on Aerospace and Electronic Systems*, vol. 46, no. 1, pp. 170–183, 2010.

[6] R. Nitzberg, "Application of maximum likelihood estimation of persymmetric covariance matrices to adaptive processing," *IEEE Transactions on Aerospace and Electronic Systems*, vol. 16, no. 1, pp. 124–127, July 1992.

[7] Y. Gao, G. Liao, S. Zhu, X. Zhang, and D. Yang, "Persymmetric adaptive detectors in homogeneous and partially homogeneous environments," *IEEE Transactions on Signal Processing*, vol. 62, no. 2, pp. 331–342, January 2014.

[8] C. Hao, D. Orlando, G. Foglia, X. Ma, S. Yan, and C. Hou, "Persymmetric adaptive detection of distributed targets in partially-homogeneous environment," *Digital signal processing*, vol. 24, no. 1, pp. 42–51, 2014.

[9] G. Pailloux, P. Forster, J.-P. Ovarlez, and F. Pascal, "Persymmetric adaptive radar detectors," *IEEE Transactions on Aerospace and Electronic Systems*, vol. 47, no. 4, pp. 2376–2390, 2011.

[10] G. Ginolhac, P. Forster, F. Pascal, and J. Ovarlez, "Exploiting persymmetry for low-rank space time adaptive processing," *Signal Processing*, vol. 97, pp. 242–251, 2014.

[11] L. Cai and H. Wang, "A persymmetric multiband GLR algorithm," *IEEE Transactions on Aerospace and Electronic Systems*, vol. 28, no. 3, pp. 806–816, 1992.

[12] J. Liu, H. Li, and B. Himed, "Persymmetric adaptive target detection with distributed MIMO radar," *IEEE Transactions on*

Aerospace and Electronic Systems, vol. 51, no. 1, pp. 372–382, 2015.

[13] G. Foglia, C. Hao, A. Farina, D. Orlando, and C. Hou, "Adaptive detection of point-like targets in partially homogeneous clutter with symmetric spectrum," *IEEE Transactions on Aerospace and Electronic Systems*, vol. 53, no. 4, pp. 2110–2119, August 2017.

[14] A. De Maio, D. Orlando, C. Hao, and G. Foglia, "Adaptive detection of point-like targets in spectrally symmetric interference," *IEEE Transactions on Signal Processing*, vol. 64, no. 12, pp. 3207–3220, June 2016.

[15] C. Hao, A. D. Maio, D. Orlando, S. Iommelli, and C. Hou, "Adaptive radar detection in the presence of Gaussian clutter with symmetric spectrum," in *ICASSP 2016*. IEEE, 2016.

[16] G. Foglia, C. Hao, G. Giunta, and D. Orlando, "Knowledge-aided adaptive detection in partially homogeneous clutter: Joint exploitation of persymmetry and symmetric spectrum," *Digital Signal Processing*, vol. 67, no. 1, pp. 131–138, 2017.

[17] C. Hao, D. Orlando, G. Foglia, and G. Giunta, "Knowledge-based adaptive detection: Joint exploitation of clutter and system symmetry properties," *IEEE Signal Processing Letters*, vol. 23, no. 10, pp. 1489–1493, 2016.

[18] I. S. Reed, J. D. Mallett, and L. E. Brennan, "Rapid convergence rate in adaptive arrays," *IEEE Transactions on Aerospace and Electronic Systems*, 1974.

[19] D. Orlando and G. Ricci, "Adaptive radar detection and localization of a point-like target," *IEEE Transactions on Signal Processing*, vol. 59, no. 9, pp. 4086–4096, 2011.

[20] C. Hao, S. Gazor, G. Foglia, B. Liu, and C. Hou, "Persymmetric adaptive detection and range estimation of a small target," *IEEE Transactions on Aerospace and Electronic Systems*, vol. 51, no. 4, pp. 2590–2604, October 2015.

[21] S. Yan, D. Massaro, D. Orlando, C. Hao, and A. Farina, "Adaptive detection and range estimation of point-like targets with symmetric spectrum," *IEEE Signal Processing Letters*, vol. 24, no. 11, pp. 1744–1748, 2017.

[22] L. Yan, C. Hao, D. Orlando, A. Farina, and C. Hou, "Parametric space-time detection and range estimation of point-like targets in partially homogeneous environment," *IEEE Transactions on Aerospace and Electronic Systems*, vol. 56, no. 2, pp. 1228–1242, 2020.

[23] A. D. Maio, C. Hao, and D. Orlando, "An adaptive detector with range estimation capabilities for partially homogeneous environment," *IEEE Signal Processing Letters*, vol. 21, no. 3, pp. 325–329, May 2014.

[24] T. Wang, C. Yin, D. Xu, C. Hao, D. Orlando, and G. Ricci, "Joint detection and delay-Doppler estimation algorithms for MIMO radars," *IEEE Transactions on Signal Processing*, vol. 72, pp. 809–823, 2024.

[25] G. Fabrizio, A. Farina, and M. Turley, "Spatial adaptive subspace detection in OTH radar," *IEEE Transactions on Aerospace and Electronic Systems*, vol. 39, no. 4, pp. 1407–1428, 2003.

[26] D. Orlando, G. Ricci, and L. L. Scharf, "A unified theory of adaptive subspace detection part I: Detector designs," *IEEE Transactions on Signal Processing*, vol. 70, pp. 4925–4938, 2022.

[27] H. L. V. Trees, *Optimum Array Processing (Detection, Estimation, and Modulation Theory, Part IV)*. Hoboken, NJ, USA: Wiley, 2002.

[28] R. Klemm, *Principles of Space-Time Adaptive Processing*. London, UK: IET, 2002.

[29] F. Bandiera, D. Orlando, and G. Ricci, *Advanced Radar Detection Schemes under Mismatch Signal Models*, Synthesis Lectures on Signal Processing No. 8, Ed. San Rafael, US: Morgan & Claypool Publishers, 2009.

[30] F. Bandiera, O. Besson, D. Orlando, G. Ricci, and L. L. Scharf, "GLRT-based direction detectors in homogeneous noise and subspace interference," *IEEE Transactions on Signal Processing*, vol. 55, no. 6, pp. 2386–2394, June 2007.

- [31] K. Duan, M. Liu, H. Dai, F. Xu, and W. Liu, "A two-stage detector for mismatched subspace signals," *IEEE Geoscience and Remote Sensing Letters*, vol. 14, no. 12, pp. 2270–2274, 2017.
- [32] C.-I. Chang, H. Cao, S. Chen, X. Shang, C. Yu, and M. Song, "Orthogonal subspace projection-based go-decomposition approach to finding low-rank and sparsity matrices for hyperspectral anomaly detection," *IEEE Transactions on Geoscience and Remote Sensing*, vol. 59, no. 3, pp. 2403–2429, 2021.
- [33] W. Liu, W. Xie, J. Liu, and Y. Wang, "Adaptive double subspace signal detection in Gaussian background-part II: Partially homogeneous environments," *IEEE Transactions on Signal Processing*, vol. 62, no. 9, pp. 2358–2369, May 2014.
- [34] D. Ciunzono, A. De Maio, and D. Orlando, "A unifying framework for adaptive radar detection in homogeneous plus structured interference- part I: On the maximal invariant statistic," *IEEE Transactions on Signal Processing*, vol. 64, no. 11, pp. 2894–2906, 2016.
- [35] D. Ciunzono, A. De Maio, and D. Orlando, "A unifying framework for adaptive radar detection in homogeneous plus structured interference- part II: Detectors design," *IEEE Transactions on Signal Processing*, vol. 64, no. 11, pp. 2907–2919, 2016.
- [36] G. Ricci and L. L. Scharf, "Adaptive radar detection of extended Gaussian targets," in *Proc. 12th Annu. Adaptive Sensor Array Process. Workshop*, vol. 1, Lexington, MA, USA, March 2004, pp. 16–18.
- [37] S. Xu, X. Shi, J. Xue, and P. Shui, "Adaptive subspace detection of range-spread target in compound Gaussian clutter with inverse Gaussian texture," *Digital Signal Processing*, vol. 81, pp. 79–89, 2018.
- [38] P. Addabbo, D. Orlando, G. Ricci, and L. L. Scharf, "A unified theory of adaptive subspace detection part II: Numerical examples," *IEEE Transactions on Signal Processing*, vol. 70, pp. 4939–4950, 2022.
- [39] A. De Maio, "Rao test for adaptive detection in Gaussian interference with unknown covariance matrix," *IEEE Transactions on Signal Processing*, vol. 55, no. 7, pp. 3577–3584, 2007.
- [40] D. Orlando and G. Ricci, "A Rao test with enhanced selectivity properties in homogeneous scenarios," *IEEE Transactions on Signal Processing*, vol. 58, no. 10, pp. 5385–5390, October 2010.
- [41] A. Coluccia, A. Fascista, and G. Ricci, "CFAR feature plane: A novel framework for the analysis and design of radar detectors," *IEEE Transactions on Signal Processing*, vol. 68, pp. 3903–3916, 2020.
- [42] S. Bose and A. O. Steinhardt, "A maximal invariant framework for adaptive detection with structured and unstructured covariance matrices," *IEEE Transactions on Signal Processing*, vol. 43, no. 9, pp. 2164–2175, 1995.
- [43] K. P. Murphy, *Machine Learning: A Probabilistic Perspective*. London UK.: The MIT Press, 2012.
- [44] L. Svensson and M. Lundberg, "On posterior distributions for signals in Gaussian noise with unknown covariance matrix," *IEEE Transactions on Signal Processing*, vol. 53, no. 9, pp. 3554–3571, 2005.
- [45] S. Bidon, O. Besson, and J.-Y. Tournet, "A Bayesian approach to adaptive detection in nonhomogeneous environments," *IEEE Transactions on Signal Processing*, vol. 56, no. 1, pp. 205–217, 2008.
- [46] N. Li, H. Yang, G. Cui, L. Kong, and Q. Huo Liu, "Adaptive two-step Bayesian MIMO detectors in compound-Gaussian clutter," *Signal Processing*, vol. 161, pp. 1–13, 2019.
- [47] P. Wang, H. Li, and B. Himed, "Knowledge-aided parametric tests for multichannel adaptive signal detection," *IEEE Transactions on Signal Processing*, vol. 59, no. 12, pp. 5970–5982, December 2011.
- [48] M. S. Greco, F. Gini, and P. Stinco, "Cognitive radars: Some applications," in *2016 IEEE Global Conference on Signal and Information Processing (GlobalSIP)*, 2016, pp. 1077–1082.
- [49] M. S. Greco, F. Gini, P. Stinco, and K. Bell, "Cognitive radars: On the road to reality: Progress thus far and possibilities for the future," *IEEE Signal Processing Magazine*, vol. 35, no. 4, pp. 112–125, 2018.
- [50] C. Yin, C. Hao, D. Orlando, and C. Hou, "Learning strategies for the interference covariance structure based on a Bayesian approach," *IEEE Signal Processing Letters*, vol. 29, pp. 1182–1186, 2022.
- [51] S. Guruacharya, B. K. Chalise, and B. Himed, "MAP ratio test detector for radar system," *IEEE Transactions on Signal Processing*, vol. 69, pp. 573–588, 2021.
- [52] A. P. Dempster, N. M. Laird, and D. B. Rubin, "Maximum likelihood from incomplete data via the EM algorithm," *J. Rou. Stat. Soc. (Series B-Methodological)*, vol. 39, no. 1, pp. 1–38, 1977.
- [53] L. Yan, S. Han, C. Hao, D. Orlando, and G. Ricci, "Innovative cognitive approaches for joint radar clutter classification and multiple target detection in heterogeneous environments," *IEEE Transactions on Signal Processing*, vol. 71, pp. 1010–1022, 2023.
- [54] A. Culocchia, A. Fascista, D. Orlando, and G. Ricci, "Adaptive radar detection in heterogeneous clutter plus thermal noise via the Expectation-Maximization algorithm," *IEEE Transactions on Aerospace and Electronic Systems*, vol. 60, no. 1, pp. 212–225, February 2024.
- [55] P. Addabbo, S. Han, D. Orlando, and G. Ricci, "Learning strategies for radar clutter classification," *IEEE Transactions on Signal Processing*, vol. 69, pp. 1070–1082, 2021.
- [56] C. Bishop, *Pattern Recognition and Machine Learning*, ser. Information Science and Statistics. Springer, 2006.
- [57] A. Yeredor, "The joint MAP-ML criterion and its relation to ML and to extended least-squares," *IEEE Transactions on Signal Processing*, vol. 48, no. 12, pp. 3484–3492, 2000.
- [58] M. A. Richards, J. A. Scheer, and W. A. Holm, *Principles of Modern Radar: Basic Principles*. Raleigh, NC: Scitech Publishing, 2010.
- [59] S. Kraut and L. L. Scharf, "The CFAR adaptive subspace detector is a scale-invariant GLRT," *IEEE Transactions on Signal Processing*, vol. 47, no. 9, pp. 2538–2541, September 1999.
- [60] E. Conte, M. Lops, and G. Ricci, "Asymptotically optimum radar detection in compound-Gaussian clutter," *IEEE Transactions on Aerospace and Electronic Systems*, vol. 31, no. 2, pp. 617–625, 1995.
- [61] J. Billingsley, A. Farina, F. Gini, M. Greco, and L. Verrazzani, "Statistical analyses of measured radar ground clutter data," *IEEE Transactions on Aerospace and Electronic Systems*, vol. 35, no. 2, pp. 579–593, 1999.

This figure "farina.jpg" is available in "jpg" format from:

<http://arxiv.org/ps/2503.02214v1>

This figure "hao.jpg" is available in "jpg" format from:

<http://arxiv.org/ps/2503.02214v1>

This figure "yan.jpg" is available in "jpg" format from:

<http://arxiv.org/ps/2503.02214v1>

This figure "yin.jpg" is available in "jpg" format from:

<http://arxiv.org/ps/2503.02214v1>